Molecular Pharmacology Fast Forward. Published on July 1, 2004 as doi:10.1124/mol.104.001784
This article has not been copyedited and formatted. The final version may differ from this version.

MOL 1784

Discovery and characterization of novel small molecule inhibitors of human Cdc25B dual specificity phosphatase.

Marni Brisson, Theresa Nguyen, Andreas Vogt, Jack Yalowich, Angela Giorgianni, Dror Tobi, Ivet Bahar, Corey R. J. Stephenson, Peter Wipf, and John S. Lazo

Department of Pharmacology and the Fiske Drug Discovery Laboratory (M.B., T.N., A.V., J.Y., A.G., J.S.L.), Department of Chemistry and the Center for Chemical Methodologies and Library Development (C.R.J.S., P.W.), and the Center for Computational Biology and Bioinformatics (D.T., I.B.), University of Pittsburgh, Pittsburgh, PA 15261-0001

Molecular Pharmacology Fast Forward. Published on July 1, 2004 as DOI: 10.1124/mol.104.001784
This article has not been copyedited and formatted. The final version may differ from this version.

MOL 1784

Running title: Cdc25B phosphatase inhibitors

Corresponding author: John S. Lazo; Department of Pharmacology, University of Pittsburgh, E1340 Biomedical Science Tower, Pittsburgh, PA 15261-0001; Fax: 412-648-2229; Email: lazo@pitt.edu

Number of text pages: 36

Number of Tables: 1

Number of Figures: 10

Number of References: 27

Number of words in Abstract: 243

Number of words in Introduction: 651

Number of words in Discussion: 921

Abbreviations: Cdk, cyclin-dependent kinase; DSPase, dual specificity phosphatase; GI_{50}, median growth inhibitory concentration; GST, glutathione S-transferase; IC_{50}, median inhibitory concentration; PTPases; tyrosine-specific protein phosphatases

Molecular Pharmacology Fast Forward. Published on July 1, 2004 as DOI: 10.1124/mol.104.001784
This article has not been copyedited and formatted. The final version may differ from this version.

ABSTRACT

Cdc25A and Cdc25B dual specificity phosphatases are key regulators of cell cycle transition and proliferation. They have oncogenic properties and are overexpressed in many human tumors. Since selective Cdc25 phosphatase inhibitors would be valuable biological tools and possible therapeutic agents, we have assayed a small molecule library for *in vitro* inhibition of Cdc25. We now report the identification of two new structurally distinct classes of Cdc25 inhibitors with cellular activity. The cyclopentaquinoline 5661118 (3a,4,5,9b-tetrahydro-1H-cyclopenta[*c*]quinoline-4,8-dicarboxylic acid) and the naphthofurandione 5169131 (3-benzoyl-naphtho[1,2-b]furan-4,5-dione) had *in vitro* IC_{50} values of 2.5-11 μM against recombinant Cdc25 and were less potent inhibitors of other phosphatases. Unlike 5661118, 5169131 caused reversible inhibition of Cdc25B and displayed competitive inhibitor kinetics. No growth inhibitory activity was seen with 5661118, while 10-30 μM 5169131 caused G_1/S and G_2/M arrest. We also found that 5169131 inhibited human PC-3 prostate and MDA-MB-435 breast cancer cell proliferation. Concentration-dependent Tyr15 hyperphosphorylation was seen on cyclin dependent kinase 1 one hour after 5169131 treatment, consistent with Cdc25 inhibition. Cells resistant to DNA toposiomerase II inhibitors were as sensitive to 5169131 as parental cells indicating that this quinone compound does not inhibit topoisomerase II *in vivo*. Molecular modeling was used to predict a potential interaction site between the inhibitor and Cdc25B and to provide insights as to the molecular origins of the experimental observations. Based on its kinetic profile and cellular activity, we suggest 5169131 could be an excellent tool for further studies on the cellular roles of Cdc25.

Molecular Pharmacology Fast Forward. Published on July 1, 2004 as DOI: 10.1124/mol.104.001784
This article has not been copyedited and formatted. The final version may differ from this version.

INTRODUCTION

Protein phosphorylation regulates mammalian cellular communication, growth and survival. Small molecule inhibitors have been valuable tools for decoding the role of various kinases and phosphatases in specific cellular signaling pathways. They are particularly attractive because, unlike most genetic approaches, they are generally reversible, produce graded responses and can easily penetrate cells. There are a growing number of small molecule inhibitors for protein kinases but potent and selective inhibitors are unavailable for some of the potentially important protein phosphatases.

Protein phosphatases are classified according to the amino acid phosphate ester that they hydrolyze and are divided into two major families, the serine/threonine-specific protein phosphatases and the tyrosine-specific protein phosphatases (PTPases). PTPases are of interest because they regulate fundamental cellular processes often perturbed in malignant cells. PTPases can be identified by the conserved motif -H-C-X_5-R- (where X is any amino acid) that makes up the active site of the enzyme's catalytic domain. Outside of this conserved active site motif, PTPases share almost no sequence homology (Denu et al., 1996). The dual specificity phosphatases (DSPases) are a sub-class of the PTPase family. They contain this conserved -H-C-X_5-R- active site motif but differ from other PTPases because they are capable of hydrolyzing phosphate ester bonds on tyrosines and threonines in the same protein substrate. Genomic studies predict that there are 29 human DSPases, with the best studied being the Cdc25 phosphatases. These phosphatases control cell cycle progression by dephosphorylating and activating cyclin-

Molecular Pharmacology Fast Forward. Published on July 1, 2004 as DOI: 10.1124/mol.104.001784
This article has not been copyedited and formatted. The final version may differ from this version.

dependent kinases (Cdk) (Lyon et al., 2002). Three human Cdc25 homologs exist: Cdc25A, Cdc25B and Cdc25C (Lyon et al., 2002). Cdc25A is involved in G_1/S phase transition, where it dephosphorylates the Cdk2/cyclin A complex (Hoffman et al., 1994) and also has a role in mitosis (Mailand et al., 2002). Cdc25A is rapidly degraded in response to DNA damage, which impairs the G_1/S transition (Mailand et al., 2000). Cdc25B is thought to function as a mitotic starter by dephosphorylating and activating Cdk2/cyclin A and Cdk1/cyclin B (Nilsson and Hoffmann, 2000). Cdc25C dephosphorylates and activates the Cdk1/cyclin B mitotic kinase complex, thus permitting cell entry into mitosis and also controlling the initiation of S-phase (Turowski et al., 2003). In addition to their prominent role in cell cycle control, the Cdc25 phosphatases are involved in mitogenic and steroid receptor signal transduction pathways and apoptotic responses to stress (Lyon et al., 2002).

Elevated levels of Cd25A and Cdc25B but not Cdc25C have been noted in many human tumor types, such as breast, ovary, colon, and head and neck, where there appears to be a remarkable association with high protein levels and either tumor aggressiveness or poor prognosis (Cangi et al., 2000; Lyon et al., 2002; Takemasa et al., 2000). Cdc25A and Cdc25B have been reported to transform cells in cooperation with the Ras oncogene or in the absence of the Retinoblastoma tumor suppressor protein (Galaktionov et al., 1995). Cdc25 B expression is increased after transformation of primary fibroblasts with SV40 large T antigen (Vogt et al., 1998) and after treatment with a human pulmonary carcinogen in human lung cells (Oguri et al., 2003). Cdc25A and B are also transcriptional targets of the c-*myc* oncogene (Galaktionov et al., 1996). Thus,

Molecular Pharmacology Fast Forward. Published on July 1, 2004 as DOI: 10.1124/mol.104.001784
This article has not been copyedited and formatted. The final version may differ from this version.

overexpression of Cdc25 phosphatases in neoplasia might provide a growth advantage through the loss of critical cell cycle checkpoint controlling mechanisms or by loss of normal apoptotic signaling mechanisms (Lyon et al., 2002). Consequently, there has been considerable interest in identifying selective, cell active inhibitors of Cdc25 phosphatases.

Thus, the current work was initiated on the belief that novel selective Cdc25 inhibitors could be obtained by using a general and unbiased *in vitro* screening approach evaluating a chemically diverse compound library enriched with compounds having drug-like properties. We describe the discovery and characterization of the naphthofuranediones, a novel class of Cdc25 inhibitors containing an *ortho*-quinoid substructure, which have inhibitory specificity, appear to be reversible, block cell cycle progression and demonstrate growth inhibitory activity against human tumor cells in culture.

Molecular Pharmacology Fast Forward. Published on July 1, 2004 as DOI: 10.1124/mol.104.001784
This article has not been copyedited and formatted. The final version may differ from this version.

MATERIALS AND METHODS

Library Chemicals. The PRIME-Collection™ compound library, which consists of 10,000 drug-like small molecules (average molecular weight = 350 Da), was obtained from Chembridge, Inc. (San Diego, CA). We have used the Chembridge compound nomenclature (namely, ID number) throughout this manuscript for compounds obtained from the vendor to facilitate their acquisition by the readers. These compounds were selected from the vendor's collection of drug-like molecules based on a three dimensional pharmacophore analysis to represent the broadest component of biologically relevant pharmacophore diversity space. Each compound was dissolved in DMSO at an average concentration of 10 μM. For some studies we used compounds kindly provided by Jill Johnson of the Developmental Therapeutic Program of the National Cancer Institute.

Synthesis of CRS-057. The diacid 5661118 (1.0 mg, 3.9 μmol) was obtained from Chembridge Inc. and dissolved in 600 μl of methanol. We then added 200 μmol of trimethylsilyl diazomethane ($TMSCHN_2$) dissolved in 100 μl of hexane and the reaction mixture was stirred for 10 min, quenched with saturated NH_4Cl solution and extracted with ethyl acetate. The combined organic layers were washed with brine, dried (Na_2SO_4) and concentrated. The residue was purified by chromatography on SiO_2 (3:1, hexanes/EtOAc), resulting in 1.1 mg of a 99% pure, colorless solid identified as 3a,4,5,9b-tetrahydro-1H-cyclopenta[c]quinoline-4,8-dicarboxylic acid dimethyl ester (CRS-057) (99% pure). Relevant ^1H NMR (C_6D_6) data: δ 7.98 (s, 1 H), 7.88 (dd, J = 8.4, 1.7 Hz, 1 H), 6.00 (d, J = 8.4 Hz, 1 H), 5.58-5.52 (m, 1 H), 5.38-5.33 (m, 1 H), 4.23 (bs,

Molecular Pharmacology Fast Forward. Published on July 1, 2004 as DOI: 10.1124/mol.104.001784
This article has not been copyedited and formatted. The final version may differ from this version.

1 H), 3.69 (d, *J* = 8.2 Hz, 1 H), 3.57 (s, 3 H), 3.26 (s, 3 H), 3.01-2.95 (m, 1 H), 2.46-2.37 (m, 1 H), 2.11-2.03 (m, 1 H), 1.35-1.22 (m, 1 H).

***In vitro* enzyme assays.** Epitope-tagged (either His_6 or GST) $Cdc25A_1$, $Cdc25B_2$, $Cdc25C_1$, were expressed in *E. coli* and purified by Ni-NTA (His_6) resin or glutathione sepharose resin (GST). Human recombinant VHR, PTP1B and bovine kidney Protein Phosphatase 2A2 was purchased from BIOMOL (Plymouth Meeting, PA). PP2A2 enzyme activity was measured using the ProFluor™ Ser/Thr phosphatase assay kit from Promega (Madison, WI). Activities of all other PTPases and DSPases were measured using the substrate O-methyl fluorescein phosphate (Sigma, St. Louis, MO) at concentrations varying with the K_m of each enzyme in a 96-well microtiter plate assay based on previously described methods (Lazo et al., 2001). The final incubation mixtures (25 μl) were prepared with a Biomek 2000 laboratory automation workstation (Beckman Coulter, Inc., Fullerton, CA). Fluorescence emission from the product was measured after a 20 or 60 min incubation period at ambient temperature with a multiwell plate reader (PerSeptive Biosystems Cytofluor II; Framingham, MA; excitation filter, 485/20; emission filter, 530/30). Best curve fit for Lineweaver-Burk plots and K_i values was determined by using the curve fitting programs Prism 3.0 (GraphPad Software, Inc., San Diego, CA) and Sigma Plot 2000, Enzyme Kinetics Module 1.0 (SPSS, Inc., Chicago, IL). For enzyme inhibition kinetics studies, we used a minimum of 6 compound concentrations and 5 substrate concentrations. Velocities were calculated by recording fluorescence readings every 5-10 min for 60 min. For studies on the reversibility of inhibitors, we used a protocol similar to a previously described dilution method (Sohn et

Molecular Pharmacology Fast Forward. Published on July 1, 2004 as DOI: 10.1124/mol.104.001784
This article has not been copyedited and formatted. The final version may differ from this version.

al., 2003). Purified Cdc25B full-length enzyme was dialyzed in 2X assay buffer (60 mM Tris, 2 mM EDTA, 150 mM NaCl, pH 8.0) before incubation with 30 μM 5169131 or 2.5 μM DA3003-1 for 0, 5 or 20 min at room temperature. Enzyme was also incubated with DMSO as a positive control. After preincubation with inhibitor or DMSO, samples were diluted 10-fold and remaining enzyme activity was determined by a phosphatase assay using O-methyl fluorescein phosphate substrate as described above.

Cdk1/cyclin B protein kinase assays were performed using purified Cdk1/cyclin B from New England Biolabs (Beverly, MA). We incubated 40U of Cdk1/cyclin B in kinase buffer (50 mM Tris-HCl, 10 mM $MgCl_2$, 1 mM EGTA, 2 mM DTT, 0.01% Brij 35, pH 7.5) containing 100 μM ATP, 10μCi [γ-^{32}P]ATP and 0.3 mg/ml Histone H1 with either DMSO vehicle, roscovitine (50 μM), or 5169131 (1-30 μM) for 30 min at 30^{o}C. A sample containing no Cdk1/cyclin B enzyme was used as a negative control. Reactions were stopped by addition of SDS electrophoresis loading buffer, followed by boiling for 5 min. Samples were resolved on a 12% Tris-glycine gel that was fixed (50% methanol, 10% acetic acid, 40% dH_2O) and dried on a BioRad model 583 gel dryer (Hercules, CA) before exposing to a phosphor screen. Radioactive bands were analyzed on a STORM™ 860 PhosphoImager (Amersham Biosciences, Piscataway, NJ).

Antiproliferative assays. The proliferation of human MDA-MD-435 breast and PC-3 prostate cells was measured by our previously described fluorescence-based assay with a Cellomics ArrayScan II (Vogt et al., 2002). Briefly, cells (1,000 per well) were plated and treated in two 384 well collagen-coated darkwell plates (Biocoat®, Becton Dickinson

Molecular Pharmacology Fast Forward. Published on July 1, 2004 as DOI: 10.1124/mol.104.001784
This article has not been copyedited and formatted. The final version may differ from this version.

Labware, Bedford, MA). After an 18 h attachment period, one plate was stained and analyzed as described below to establish cell densities at time of treatment. The other plate was treated with various concentrations of 5169131 or vehicle (DMSO) and incubated for an additional 96 h in a humidified atmosphere of 5% CO_2 at 37°C. Cells were stained with 2 µg/ml Hoechst 33342 in complete growth medium, fixed with 6% formaldehyde for 10 min at room temperature and washed twice with PBS. Plates were sealed and cells were enumerated on an ArrayScan II HCS reader (Cellomics, Pittsburgh, PA).

Three images per well were acquired using an Omega XF93 filter set at excitation/emission wavelengths of 350/461 nm. A nuclear mask was generated from images of Hoechst 33342-stained nuclei, and object identification thresholds and shape parameters were set such that the algorithm identified over 90% of the nuclei in each field. Objects that touched each other or the edge of the image were excluded from the analysis. The number of cells per field was determined by enumerating objects in the Hoechst channel. Using this methodology, typical cell densities for vehicle-treated cells at the beginning and at the end of the study ranged from 10-40 cells per field and 150-400 cells per field, respectively. The GI_{50} was defined as the concentration of drug that inhibited cell expansion over 4 days by 50%.

Human leukemia K562 and K/VP.5 cells were grown in suspension, plated in 24 well plates at a concentration of 1.5-1.7 x 10^5 cells/ml, and incubated with various concentrations of 5169131 for 48 h, after which cells were counted on a model ZBF

Molecular Pharmacology Fast Forward. Published on July 1, 2004 as DOI: 10.1124/mol.104.001784
This article has not been copyedited and formatted. The final version may differ from this version.

Coulter counter (Coulter Electronics, Hialeah, FL). The IC_{50} growth-inhibitory concentration for each cell line was calculated from a non-linear least squares fit to a four parameter logistic equation.

Flow cytometry. tsFT210 cells are a temperature sensitive Cdk1 mutant cell line isolated from the mouse mammary carcinoma cell line FM3A (Osada et al., 1997). tsFT210 cells were plated at 0.5-1 x 10^6 cells/ml, maintained at the permissive temperature of 32.0°C in a humidified atmosphere of 5% CO_2 and treated as previously described (Pu et al., 2002). Briefly, cell proliferation was arrested at the G_2/M transition by incubation at 39.4°C for 17 h. To probe for reinforcement of the G_2/M arrest induced by the compounds, we incubated cells at 32.0°C in the presence of various concentrations of 5169131, 5661118, nocodazole or DMSO vehicle for 6 h. To probe for G_1 arrest induced by the compounds, we incubated temperature-arrested cells (at G_2/M) at the permissive temperature (32^{o}C) for 4-6 h followed by treatment of these G_1 synchronized cells for 6 h with various concentrations of 5169131, 5661118, roscovitine or DMSO. Asynchronous cells were treated for 24 h. Cells were harvested with phosphate buffered saline, fixed in ice-cold 70% ethanol overnight at –20^{o}C, washed twice in phosphate buffered saline and stained with 500 µl of propidium iodide/Rnase staining buffer per 1x10^6 cells (BD Pharmingen, San Diego, CA). Flow cytometry was conducted on a FACSCalibur flow cytometer (BD Pharmingen, San Diego, CA) and data was analyzed using ModFit LT cell-cycle analysis software (Verity Software House, Topsham, ME).

Molecular Pharmacology Fast Forward. Published on July 1, 2004 as DOI: 10.1124/mol.104.001784
This article has not been copyedited and formatted. The final version may differ from this version.

Immunoprecipitation and western blotting. tsFT210 cells were arrested in G_2/M by incubation at 39.4°C for 17 h. We then added 5169131 (1-30 μM) or DMSO vehicle to cells for 1 h at 32°C. Cells were suspended and vortexed every 10 min in ice-cold lysis buffer (50 mM Tris HCl, pH 7.5, containing 250 mM NaCl, 5 mM EDTA, and 0.1% Triton X-100) supplemented with various protease and phosphatase inhibitors. Total protein concentration was determined by Bradford assay (Bio-Rad, Hercules, CA) and lysates were incubated with 50 μl of an anti-Cdc2 p34 IgG_{2A} mouse monoclonal antibody-agarose conjugate (Santa Cruz Biotechnology, Santa Cruz, CA) overnight at 4°C on an orbital rocker. Immunocomplexes were washed three times in ice-cold phosphate buffered saline supplemented with protease and phosphatase inhibitors. Immunocomplexes were boiled in SDS electrophoresis loading buffer and supernatants were resolved on a 12% Tris-glycine gel. Proteins were transferred to a nitrocellulose membrane and blotted with anti-phospho-Cdc2 (Tyr15) rabbit polyclonal antibody (Cell Signaling Technology, Beverly, MA) for detection of hyperphosphorylated Cdk1. Membranes were stripped and reprobed with an anti-Cdk1 mouse monoclonal antibody (Santa Cruz Biotechnology) for detection of total levels of Cdk1 (loading control). To examine cellular Cdc25A inhibition, we transfected HeLa cells with a cytomegalovirus promoter-driven plasmid encoding an HA epitope tagged Cdc25A (CMV-HA-Cdc25A) and treated 24 h later with vehicle or 5169131 (20 or 30 μM) for 2 h. The ectopically expressed Cdc25A was immunoprecipitated with an anti-HA.11 mouse monoclonal antibody (Covance, Berkeley, CA) and Cdc25A activity was determined by our *in vitro* OMFP assay similar to methods previously described (Brezak et al., 2004; Turowski et al., 2003).

Molecular Pharmacology Fast Forward. Published on July 1, 2004 as DOI: 10.1124/mol.104.001784
This article has not been copyedited and formatted. The final version may differ from this version.

Molecular modeling studies. The deposited crystal structure of the catalytic subunit of Cdc25B (PDB code 1QB0) (Reynolds et al., 1999) served as the structural basis for modeling of the complexes Cdc25B/5169131 and Cdc25B/OMFP. All calculations were carried out with the MOE software package (Chemical Computing Group Inc., Montreal, Quebec). Docking simulations were carried out using the MMFF94 force field (Halgren, 1996) and implicit solvation model. Docking of the inhibitor to Cdc25B was performed using the MOE-Docked subroutine. The inhibitor was placed within the catalytic loop (His472 – Arg479) and a relatively large docking box (78 x 73 x 57$Å_3$) was defined around the inhibitor to include any possible binding site. Using a simulated annealing search protocol, 70 docking runs were performed starting each time from a random position within the docking box at an initial temperature of 1000K. The docking simulations were carried out on a Xeon 3.0 GH Dell workstation during a ten day period. Low energy conformations were further refined by energy minimization using the MMFF94s force field and implicit solvation model until the norm of the gradient was less than or equal to 0.1 kcal mol^{-1} $Å^{-1}$. A model for the Cdc25B/OMFP complex was formed by overlapping the phosphate group of OMFP with the sulfate group bound to the catalytic loop of Cdc25B. Three possible overlap orientations were tested (based on the 120^0 symmetry of the sulfate oxygen atoms). The energies of the resulting complexes were minimized and the lowest energy conformation was selected.

Molecular Pharmacology Fast Forward. Published on July 1, 2004 as DOI: 10.1124/mol.104.001784
This article has not been copyedited and formatted. The final version may differ from this version.

RESULTS

Twenty-three compounds in our initial chemical library of 10,000 compounds were found to inhibit recombinant full length human Cdc25B with IC_{50} values of 10 μM or less. Two compounds, 5661118 (Figure 1) and 5169131 (Figures 3), were selected for further analysis due to their unique core chemical structures, which had not previously been reported to have antiphosphatase activity. The dicarboxylated cyclopentaquinoline 5661118 (Figure 1) had IC_{50} values against Cdc25B, VHR and PTP1B of 2.5 ± 0.1, >100 and 6.6 ± 0.1 μM, respectively. With the catalytic domain of Cdc25A, we found 5661118 had an IC_{50} of 5.4 μM and exhibited mixed partial competitive inhibition with an apparent K_i of 9.0 ± 1.9 μM (SEM; N=3) (Figure 2). We probed for structural features important for Cdc25 inhibition in the original 10,000 compound library screen by searching for compounds with the cyclopentaquinoline substructure and identified 5654435, 5660797 and 5729543 (Figure 1). We obtained additional cyclopentaquinolines from the company's master library and from the National Cancer Institute's Chemical Repository, which we had previously studied (Lazo et al., 2001; Lazo et al., 2002). The only cyclopentaquinoline with similar inhibitory effects was the diacid 5654435 (Cdc25B IC_{50}=4.5 μM). Compound 5660797 demonstrated that replacement of one acid moiety in 5654435 with chlorine caused a six-fold increase in IC_{50} value for Cdc25B. The uniqueness of 5661118 was further illustrated by the lack of any detectable Cdc25B inhibitory activity with other related compounds (namely, 5729543, NSC 627021, NSC 604519 and NSC 655442) at 100 μM (Figure 1). Because Cdc25 phosphatases have a central role in controlling cell cycle progression, we further evaluated the ability of

Molecular Pharmacology Fast Forward. Published on July 1, 2004 as DOI: 10.1124/mol.104.001784
This article has not been copyedited and formatted. The final version may differ from this version.

5661118 to arrest cell cycle progression at the G_2/M phase with our previously described tsFT210 cells (Pu et al., 2002). While the positive control compound nocodazole caused clear G_2/M arrest, concentrations $\geq$ 30 μM of 5661118 had no noticeable effect on cell cycle progression (data not shown). We synthesized the diester derivative of 5661118, CRS-057, to enhance possible cell entry but this compound had no *in vitro* inhibitory activity against Cdc25B at 100 μM, further emphasizing the importance of the diacid motif for inhibitory activity. When we tested the cell cycle effects of the diester analog CRS-057, which theoretically should more readily enter cells and be trapped due to esterase cleavage, we observed no G_2/M phase arrest (data not shown). Although we cannot exclude the possibility that CRS-057 failed to enter cells or was not de-esterified within the tsFT210 cells, we elected to focus our efforts on the naphthofurandiones, described in detail below, because of their lack of PTP1B inhibitory activity and the apparent reversibility of Cdc25 inhibition.

The naphthofurandione 5169131 (Figure 3A) had an IC_{50} against Cdc25B of 10.4 μM ± 0.1 and IC_{50} values against Cdc25A and Cdc25C of 5 μM ± 0.1 and 8.8 μM ± 0.1 (SEM; N=8) (Figure 3B). This compound also demonstrated considerable specificity for Cdc25 dual specificity phosphatases as reflected by the lack of significant inhibition of VHR and PP2A2 (IC_{50} > 100 μM) and PTP1B (IC_{50} = 67.0 μM ± 0.1) (SEM; N=8). An additional naphthofurandione, 5169133, was found in the 10,000 compound library and it was evaluated for inhibition of Cdc25A, B and C (Figure 3A and C). This brominated analog of 5169131 was markedly less effective as a phosphatase inhibitor with IC_{50} values

Molecular Pharmacology Fast Forward. Published on July 1, 2004 as DOI: 10.1124/mol.104.001784
This article has not been copyedited and formatted. The final version may differ from this version.

against Cdc25A, Cdc25B, and Cdc25C of 57.5 ± 0.1, 58.7 ± 0.1 and 41.1 ± 0.1 μM (SEM; N=4), respectively.

Kinetic studies with 5169131 and Cdc25B revealed a competitive inhibition profile with an apparent K_i of 4.5 ± 0.6 μM (range; N=2) (Figure 4A). To assess the reversibility of Cdc25B inhibition, we used a previously described dilution method (Sohn et al., 2003) in which the enzyme is pre-incubated for various times with a high concentration of a putative inhibitor in the absence of the substrate, followed by 10-fold dilutions of the enzyme and inhibitor before assaying for remaining enzyme activity. An irreversible inhibitor would be expected to cause time-dependent inhibition of the enzyme in excess of that seen with enzyme that was not pre-incubated with the inhibitor. Conversely, a reversible inhibitor should have no effect on enzyme activity when pre-incubated with the enzyme. Cdc25B was pre-incubated for 0, 5 min and 20 min with a concentration of 5169131 (30 μM) that was 3-fold greater than the IC_{50} or with the DMSO vehicle control to determine the remaining enzyme activity after compound dilution (Figure 4B). We also pre-incubated the enzyme with DA3003-1, a previously described (Lazo et al., 2001) irreversible *para*-quinone inhibitor known to form covalent adducts with Cdc25 (Pu et al., 2002) at ≥3 times the IC_{50} concentrations (2.5 μM) for the same time periods. Pre-incubation of Cdc25B with the irreversible inhibitor DA3003-1 for 0 and 5 min resulted in 65-70% reduction in phosphatase activity. After a 20 min pre-incubation, a time-dependent reduction in enzyme activity was observed with ~90% of the enzyme activity inhibited by DA3003-1 (Figure 4B). In contrast, we found that pre-incubation of Cdc25B with 5169131 did not irreversibly inhibit Cdc25B (Figure 4B).

Molecular Pharmacology Fast Forward. Published on July 1, 2004 as DOI: 10.1124/mol.104.001784
This article has not been copyedited and formatted. The final version may differ from this version.

Because of the promising *in vitro* results we observed with 5169131, we next examined the cellular actions of the inhibitor. We first tested the ability of 5169131 to arrest cells at the G_2/M phase of the cell cycle, since an inhibitor of Cdc25 should block cell cycle progression. Incubation of tsFT210 cells at the restrictive temperature of 39.4^{o}C for 17 h resulted in G_2/M arrest (Figure 5, Panel B; Table 1A). We then released the synchronized cells in the presence of 1-30 μM 5169131 for 6 h at 32^{o}C (Figure 5, Panels E-H). When compared to cells treated with the vehicle control (Figure 5, Panel C), cells exposed to 5169131 clearly demonstrated a concentration-dependent G_2/M arrest consistent with inhibition of the Cdc25 phosphatase family (Figure 5, Panels E-H; Table 1A). Cells treated with 20 or 30 μM 5169131 showed G_2/M arrest, which began to approach that seen with nocodazole treated control cells (Figure 5, Panel D). These compound concentrations were also cytotoxic, resulting in 20% and 50% cell death, respectively, base on Trypan Blue dye exclusion (data not shown). A small amount of G_2/M arrest was still apparent with 10 μM of inhibitor (Figure 5, Panel F; Table 1A). Interestingly, a pre-G_1 peak indicative of an apoptotic cell population was apparent with 10-30 μM inhibitor concentrations. The toxicity and pre-G_1 peaks observed at the highest compound concentrations could be indicative of apoptotic death induced by 5169131; however, the exact mechanisms of cell death have yet to be determined. The percentage of cells at each phase of the cell cycle under the various treatments is presented in Table 1A.

Molecular Pharmacology Fast Forward. Published on July 1, 2004 as DOI: 10.1124/mol.104.001784
This article has not been copyedited and formatted. The final version may differ from this version.

Inhibition of Cdc25A, B, and/or C should not only induce a G_2/M arrest, but also should cause Cdk1 hyperphosphorylation. Thus, we arrested tsFT210 cells at G_2/M, followed by exposure to various concentrations of 5169131 or DMSO vehicle control for 1 h. The cells were lysed and immunoprecipitated with an anti-Cdk1 mouse monoclonal antibody. Proteins were transferred to nitrocellulose membranes and immunoblotted with an anti-phospho-Cdk1 (Tyr15) antibody. Treatment with 5169131 resulted in a concentration-dependent increase in Cdk1 hyperphosphorylation (Figure 6A). When the phospho-Cdk1 levels with each treatment were normalized to the total Cdk1 levels by densitometry and compared to DMSO treated cells, we found 1.6, 2.6 and 4.5 fold increases in phospho-Cdk1 with 10, 20 and 30 μM 5169131, respectively. The levels of hyperphosphorylation corresponded to the concentration-dependent increase in G_2/M arrest seen in Figure 5. Cells treated with the DMSO vehicle continued to progress past G_2/M, resulting in no hyperphosphorylation of Cdk1. These results are consistent with what would be expected of an inhibitor of Cdc25 phosphatases. The G_2/M arrest caused by 5169131 could not be ascribed to the direct inhibition of Cdk1 kinase activity because 5169131 (1-30 μM) had no significant inhibitory effect on purified Cdk1/cyclin B kinase using Histone H1 as a substrate as compared to vehicle control (Figure 6B). In contrast roscovitine, a non-specific inhibitor of cyclin dependent kinases, significantly reduced Cdk1/cyclin B kinase activity.

Because 5169131 exhibited *in vitro* Cdc25A inhibitory activity, we also probed whether or not the compound could cause a G_1 phase arrest. Thus, G_2/M arrested tsFT210 cells (Figure 7, Panel B) were released into G_1 by incubating cells at the permissive 32^{o}C

Molecular Pharmacology Fast Forward. Published on July 1, 2004 as DOI: 10.1124/mol.104.001784
This article has not been copyedited and formatted. The final version may differ from this version.

temperature. After 4-6 h, almost 60% of the cells were in the G_1 phase (Figure 7, Panel C; Table 1B). We then added 1-30 μM 5169131 and incubated cells at the permissive temperature for an additional 6 h (Figure 7, Panels F-I; Table 1B). When compared to cells incubated with the DMSO vehicle control (Figure 7, Panel D; Table 1B), cells treated with 20 or 30 μM 5169131 exhibited a pronounced G_1 arrest (Figure 7, Panel H-I), which approximated the inhibition seen with 50 μM of roscovitine (Figure 7, Panel E). We observed a smaller G_1 arrest with 1 and 10 μM 5169131 compared to DMSO control cells (Figure 7, Panel F-G). It is also notable that the pre-G_1 apoptotic peak seen with 5169131-induced G_2/M arrested cells (Figure 5) was not apparent in the G_1 arrested cells at any of the 5169131 concentrations tested. Moreover, unlike the G_2/M arrested cells, no toxicity was observed with a Trypan blue exclusion assay at any of the concentrations of 5169131 tested in the G1 arrested cells. The percentage of cells at each phase of the cell cycle under the various treatments is presented in Table 1B.

G_1 arrest induced by 5169131 could be due to direct inhibition of Cdc25A in cells. To investigate this hypothesis, Hela cells transfected with a CMV-HA-Cdc25A plasmid construct were exposed to DMSO vehicle or 5169131 at 20 and 30 μM for 2 h. Using an approach that emulates one previously described (Brezak et al., 2004; Turowski et al., 2003), we immunoprecipitated cell lysates with an anti-HA.11 mouse monoclonal antibody (Covance, Berkeley, CA) and assayed for remaining Cdc25A activity using our *in vitro* enzyme assay with OMFP as a substrate (see Materials and Methods). We found 20 and 30 μM 5169131 inhibited ectopic Cdc25A activity by 57.6% and 100%, respectively, as compared to DMSO vehicle control. These results suggested that

Molecular Pharmacology Fast Forward. Published on July 1, 2004 as DOI: 10.1124/mol.104.001784
This article has not been copyedited and formatted. The final version may differ from this version.

5169131 could directly inhibit cellular Cdc25A and provide a basis for the G_1 arrest observed in Figure 7.

Because cell death was apparent in tsFT210 cells after treatment with 5169131, we examined cell proliferation of human PC-3 prostate and MDA-MD-435 breast cancer cells in the presence of increasing concentrations of the Cdc25 inhibitor (0.1 – 100 μM). Both of these cell lines express Cdc25A, Cdcd25B and Cdc25C (data not shown). 5169131 indeed inhibited cell growth at GI_{50} concentrations of 6.5 μM for PC-3 cells and 1.2 μM for MDA-MB-435 cells (Figure 8A).

A number of napthoquinones, including the *ortho*-quinone β-lapachone, have previously been found to inhibit topoisomerase IIα, resulting in increased DNA damage (Frydman et al., 1997; Wang et al., 2001). To assess whether or not the cellular effects of 5169131 were the result of inhibition of topoisomerase IIα, we examined the growth inhibition of 5169131 in two additional cell lines: parental K562 cells and KVP.5 cells, which have altered levels of topoisomerase IIα. KVP.5 cells express less topoisomerase IIα than the K562 cell line and are resistant to VP-16 and other DNA topoisomerase II poisons (Ritke et al., 1994). Both of these cell lines, however, express Cdc25 phosphatases. As seen in Figure 8B, 5169131 induced growth inhibition in both KVP.5 and K562 cells with similar IC_{50} values of 1.1 μM and 1.5 μM. Therefore, inhibition of cell proliferation by 5169131 did not appear to be due to inhibition or poisoning of DNA topoisomerase II in a cellular context.

Molecular Pharmacology Fast Forward. Published on July 1, 2004 as DOI: 10.1124/mol.104.001784
This article has not been copyedited and formatted. The final version may differ from this version.

Finally, we interrogated possible sites of interaction for 5169131 with Cdc25B by molecular modeling. Using previously published coordinates (Reynolds et al., 1999), we performed docking simulations to predict the most energetically favorable binding site of 5169131. The inhibitor was found to bind within the groove that extends from the catalytic loop of Cdc25B (Figure 9A). This groove contains the residues 427, 428, 442-448, 479 and 531-550.

To investigate the potential of competitive binding between 5169131 and the OMFP substrate, we explored possible positions and orientations of OMFP with the catalytic domain of Cdc25B. The phosphate group of OMFP was positioned to occupy the same location as the sulfate ion bound to the catalytic site of the crystal structure. The binding orientation of the sulfate group is identical to the one observed in other PTPase structures and is thought to mimic the symmetry of the sulfate oxygens. Energy minimization of the resulting complexes yielded the orientation shown in Figure 9A. The figure illustrates the superposition of the models for 5169131 and OMFP, which reveals a steric interference between these two moieties at the catalytic site of the enzyme. This could explain the competitive nature of the 5169131 inhibitor seen in the kinetic studies in Figure 4.

Further examination of the model of 5169131 with Cdc25B points to individual amino acids of the enzyme that might interact with the inhibitor. Figure 9B shows that the upper inner wall of the binding cavity is hydrophobic (shown in green). This part of the cavity is composed of the amino acids L445, F543 and Y428, which could form hydrophobic

Molecular Pharmacology Fast Forward. Published on July 1, 2004 as DOI: 10.1124/mol.104.001784
This article has not been copyedited and formatted. The final version may differ from this version.

interactions with the benzene ring of 5169131. Figure 10A demonstrates how the naphthoquinone rings in 5169131 could be stacked between the two guanidinium side chains of R482 and R544, forming favorable interactions. In addition, the model predicts that the phenolic hydroxyl group of Y428 should be located above the center of the naphthoquinone rings and forms hydrogen π interactions.

The inhibitor 5169133 is a markedly less potent congener of 5169131, containing a single bromide atom (Figure 3). Interestingly, when we modeled 5169133 with the Cdc25B catalytic domain (Figure 10B), we found the napthoquinone rings of 5169133 could also directly interact with the side chains of R482 and R544 but the bromide would sterically clash with T547, having only a 2.41 Å distance between the bromide atom and the Cγ atom of T547. Hence, this model provided a potential explanation for the difference in potency observed between 5169131 and 5169133 with respect to the Cdc25B target enzyme.

Molecular Pharmacology Fast Forward. Published on July 1, 2004 as DOI: 10.1124/mol.104.001784
This article has not been copyedited and formatted. The final version may differ from this version.

DISCUSSION

Discovery of potent, reversible and selective inhibitors of Cdc25 phosphatases should facilitate the elucidation of biological substrates and functions for these enzymes. Furthermore, potential inhibitors may prove to be useful in targeted cancer therapies due to the oncogenic nature of Cdc25A and Cdc25B in cancer cell lines. Although crystal structures for the catalytic domain of Cdc25A and Cdc25B have been published (Fauman et al., 1998; Reynolds et al., 1999), neither revealed the nature of interactions with small molecule inhibitors. Moreover, the phosphatase substrate may initiate key conformational changes and provide an important catalytic acid (Chen et al., 2000; Slack et al., 2001). This has hampered attempts to design potential inhibitors. Consequently, there are only a modest number of known DSPase inhibitors and almost all were identified using *in vitro* screening methods with artificial substrates. Inhibitors derived from natural products, such as dnacin B_1, dysidiolide, menadione, and coscinosulphate, are either irreproducible, weak, nonspecific, or form irreversible adducts with Cdc25 (Lyon et al., 2002). Other synthetic compounds based on Ser/Thr phosphatase inhibitors, dipeptidyl phosphonates or steroidal structures are either not potent or fail to enter cells effectively (Lyon et al., 2002). To date, some of the most potent and selective Cdc25 inhibitors contain *para*-quinone moieties. Compounds, such as the *para*-quininolinediones (Lazo et al., 2001) and the *para*-naphthoquinones (Lazo et al., 2002), exhibit mixed inhibition kinetics and are irreversible inhibitors (Pu et al., 2002). Others, such as the *para*-indolyldihydroxyquinones, are potent, reversible inhibitors of Cdc25B *in vitro*, but do not appear to block intracellular Cdc25 based on their failure to induce cell cycle arrest or affect cellular Cdk phosphorylation status (Sohn et al., 2003).

Molecular Pharmacology Fast Forward. Published on July 1, 2004 as DOI: 10.1124/mol.104.001784
This article has not been copyedited and formatted. The final version may differ from this version.

We have described herein two novel structural classes of Cdc25B inhibitors: the cyclopentaquinolines and the naphthofurandiones (Figures 1 and 3). Although the potency of these compounds against Cdc25 phosphatases (IC_{50} ~ 2.5-11 μM) was less than that of several previously described inhibitors, the naphthofurandiones displayed many of the attributes of a useful inhibitor lacking in the more potent compounds. For example, 5169131 showed high selectivity with no *in vitro* inhibition at 100 μM against the dual specificity phosphatase VHR and the Ser/Thr phosphatase PP2A2, and low inhibition of the tyrosine phosphatase PTP1B (IC_{50} = 67 μM). The data in Figure 4 also demonstrated that 5169131 is both a competitive and reversible inhibitor of Cdc25B. This is important because, until recently, competitive and reversible inhibitors of Cdc25 dual specificity phosphatases had not been available. The only competitive, reversible Cdc25 inhibitors reported to date are the indolyldihydroxyquinones: 2,5-dihydroxy-3-(7-farnesyl-1H-indol-3-yl)[1,4]benzoquinone and 2,5-dihydroxy-3-(4,6-dichloro-7-farnesyl-1H-indol-3-yl)[1,4]benzoquinone (Sohn et al., 2003). Although these two compounds were more potent than 5169131 with an *in vitro* K_i against the catalytic domain of Cdc25B of 640 and 470 nM, respectively, they were ineffective in cellular assays. The authors attribute their cellular ineffectiveness to significant nonspecific binding of bovine serum albumin in the serum used to culture cells (Sohn et al., 2003). Thus, we tested the effect of increasing concentrations of bovine serum albumin (0.03-0.6% weight/volume) on 5169131 inhibition of Cdc25B activity *in vitro* and found no effect (data not shown). This encouraged us to examine 5169131 in a cellular context.

Molecular Pharmacology Fast Forward. Published on July 1, 2004 as DOI: 10.1124/mol.104.001784
This article has not been copyedited and formatted. The final version may differ from this version.

5169131 inhibited the proliferation of murine tsFT210 mammary carcinoma cells, human MDA-MD-435 breast, human PC-3 prostate cancer cells and human leukemia K562 cells (Figure 8). Induction of G_2/M arrest in synchronized tsFT210 cells (Figure 5) coincided with hyperphosphorylation of Cdk1 consistent with a direct effect on the Cdc25 phosphatases (Figure 6). When we evaluated the effects of 5169131 on the cell cycle distribution in asynchronous tsFT210 cells, we found no significant difference in the cell cycle profile compared to the DMSO treated control cells. We did, however, note that after exposure to 20 or 30 μM 5169131, 25% and 80% of cells were dead based on Trypan Blue exclusion (data not shown). The failure to detect differences in the cell cycle profile of asynchronous cells could be due to the inhibition of all Cdc25 phosphatases with the prolonged compound exposure, which would lead to inactivation of all cyclin dependent kinases and blockage at G_1/S, S and G_2/M phases of the cell cycle. Alternatively, asynchronous cells may be less sensitive to growth inhibition than synchronized cells. Similar differences in compound sensitivity have been seen between asynchronized and synchronized cells by other investigators using the tsFT210 cells with the serine/threonine phosphatase inhibitor tautomycin and the Cdk1 inhibitor sangivamycin (Osada et al., 1997). The biochemical basis for this interesting difference between asynchronous and synchronous populations is not currently known.

We also attempted to model the interactions between 5169131 or the OMFP substrate with the catalytic domain of the Cdc25B enzyme (Figure 9A). The overlapping of these models demonstrated a competition between 5169131 and OMFP binding to Cdc25B. These results support the competitive inhibitor kinetic profile that we found for 5169131

(Figure 4). It appears based on the model in Figure 10A that 5169131 interacts with the residues R482 and R544 of Cdc25B. Interestingly, these same amino acids have been reported to interact with our irreversible, *para*-quinone inhibitors NSC95397 and NSC663284 (Lazo et al., 2002). Hence, this model could be tested in the future by mutating both R482 and R544. After modeling the halogenated 5169131 congener, 5169133, with Cdc25B, we found the more bulky and electron negative bromine appears to encounter severe steric interference with the neighboring T547 amino acid on Cdc25B, consistent with its decreased potency (Figure 3C & 10B). Therefore, the modeling results provided a rationale for the *in vitro* observations with 5169131 and might be useful for the design of new synthetic analogs.

Molecular Pharmacology Fast Forward. Published on July 1, 2004 as DOI: 10.1124/mol.104.001784
This article has not been copyedited and formatted. The final version may differ from this version.

ACKNOWLEDGMENTS

We are very grateful for the technical assistance of John Skoko, Rachel Sikorski, Kathleen Cooley and Eileen C. Southwick. We also thank Jill Johnson of the Developmental Therapeutics Program of the National Cancer Institute for generously providing compounds.

Molecular Pharmacology Fast Forward. Published on July 1, 2004 as DOI: 10.1124/mol.104.001784
This article has not been copyedited and formatted. The final version may differ from this version.

REFERENCES

Brezak M-C, Quaranta M, Mondésert O, Galcera M-O, Lavergne O, Alby F, Cazales M, Baldin V, Thurieau C, Harnett J, Lanco C, Kasprzyk PG, Prevost GP and Ducommun B (2004) A novel synthetic inhibitor of Cdc25 phosphatases: BN82002. *Cancer Res.* **64**:3320-3325.

Cangi MG, Cukor B, Soung P, Signoretti S, Moreira G, Ranashinge M, Cady B, Pagano M and Loda M (2000) Role of Cdc25A phosphatase in human breast cancer. *J. Clin. Invest.* **106**:753-761.

Chen W, Wilborn M and Rudolph J (2000) Dual-specific Cdc25B phosphatase: in search of the catalytic acid. *Biochemistry* **39**:10781-10789.

Denu JM, Stuckey JA, Saper MA and Dixon JE (1996) Form and function in protein dephosphorylation. *Cell* **87**:361-364.

Fauman EB, Cogswell JP, Lovejoy B, Rocque WJ, Holmes W, Montana VG, Piwnica-Worms H, Rink MJ and Saper MA (1998) Crystal structure of the catalytic domain of the human cell cycle control phosphatase, Cdc25A. *Cell* **93**:617-625.

Frydman B, Marton LJ, Sun JS, Neder D, Witiak DT, Liu AA, Wang H-M, Mao Y, Wu H-Y, Sanders MM and Liu LF (1997) Induction of DNA topoisomerase II-mediated DNA cleavage by β-lapachone and related naphthoquinones. *Cancer Res.* **57**:620-627.

Galaktionov K, Chen X and Beach D (1996) Cdc25 cell-cycle phosphatase as a target of c-myc. *Nature* **382**:511-517.

Galaktionov K, Lee AK, Eckstein J, Draetta G, Meckler J, Loda M and Beach D (1995) CDC25 phosphatases as potential human oncogenes. *Science* **269**:1575-7.

Halgren TA (1996) Merk molecular force field.1. Basis, form, scope, parameterization, and performance of MMFF94. *J. Comp. Chem* **14**:490-519.

Hoffman I, Draetta G and Karsenti E (1994) Activation of the phosphatase activity of human cdc25A by a cdk2-cyclin E dependent phosphorylation at the G1/S transition. *EMBO J.* **13**:4302-4310.

Lazo JS, Aslan DC, Southwick EC, Cooley KA, Ducruet AP, Joo B, Vogt A and Wipf P (2001) Discovery and biological evaluation of a new family of potent inhibitors of the dual specifity protein phosphatase Cdc25. *J. Med. Chem.* **44**:4042-4049.

Lazo JS, Nemoto K, Pestell KE, Cooley K, Southwick EC, Mitchell DA, Furey W, Gussio R, Zaharevitz DW, Joo B and Wipf P (2002) Identification of a potent and selective pharmacophore for Cdc25 dual specificity phosphatase inhibitors. *Molec. Pharmacol.* **61**.

Lyon MA, Ducret AP, Wipf P and Lazo JS (2002) Dual-specificity phosphatases as targets for antineoplastic agents. *Nature Rev. Drug Discov.* **1**:961-976.

Mailand N, Falck J, Lukas C, Syljuåsen RG, Welcker M and Lukas J (2000) Rapid destruction of human Cdc25A in response to DNA damage. *Science* **288**:1425-1429.

Mailand N, Podtelejnikov AV, Groth A, Mann M, Bartek J and Lukas J (2002) Regulation of G2/M events by Cdc25A through phosphorylation-dependent modulation of its stability. *EMBO J.* **21**.

Nilsson I and Hoffmann I (2000) Cell cycle regulation by the Cdc25 phosphatase family. *Prog. Cell Cycle Res.* **4**:107-114.

Oguri T, Singh SV, Nemoto K and Lazo JS (2003) The carinogen (7*R*,8*S*)-dihydroxy-(9*S*,10*R*)-epoxy-7,8,9,10-tetrahydrobenzo[*a*]pyrene induces Cdc25B expression in human bronchial and lung cancer cells. *Cancer Res.* **63**:771-775.

Osada H, Cui CB, Onose R and Hanaoka F (1997) Screening of cell cycle inhibitors from microbial metabolites by a bioassay using a mouse cdc2 mutant cell line, tsFT210. *Bioorg. Med. Chem.* **5**:193-203.

Pu L, Amoscato AA, Bier ME and Lazo JS (2002) Dual G1 and G2 phase inhibition by a novel, selective Cdc25 inhibitor 7-chloro-6-(2-morpholin-4-ylethylamino)-quinoline-5,8-dione. *J. Mol. Biol.* **293**:559-568.

Reynolds RA, Yem AW, Wolfe CL, Deibel MR, Chidester CG and Watenpaugh KD (1999) Crystal structure of the catalytic subunit of Cdc25B required for G2/M phase transition of the cell cycle. *J. Mol. Biol.* **293**:559-568.

Ritke MK, Roberts D, Allan WP, Raymond J, Bergoltz VV and Yalowich JC (1994) Altered stability of etoposide-induced topoisomerase II/DNA complexes in resistant human leukemia K562 cells. *Br. J. Cancer* **69**:687-697.

Slack DN, Seternes OM, Gabrielsen M and Keyse SM (2001) Distinct binding determinants for ERK2/p38alpha and JNK map kinases mediate catalytic activation and substrate selectivity of MAP kinase phosphatase-1. *J. Biol. Chem.* **276**:16491-16500.

Sohn J, Kiburz B, Li Z, Deng L, Safi A, Pirrung MC and Rudolph J (2003) Inhibition of Cdc25 phosphatases by indoyldihyroxyquinones. *J. Med. Chem.* **46**:2580-2588.

Takemasa I, Yamamoto H, Sekimoto M, Ohue M, Noura S, Miyake Y, Matsumoto T, Aihara T, Tomita N, Tamaki Y, Sakita I, Kikkawa N, Matsuura N, Shiozaki H

and Monden M (2000) Overexpression of CDC25B phosphatase as a novel marker of poor prognosis of human colorectal carcinoma. *Cancer Res.* **60**:3043-3050.

Turowski P, Franckhauser C, Morris MC, Vaglio P, Fernandez A and Lamb NJ (2003) Functional Cdc25C dual-specificity phosphatase is required for S-phase entry in human cells. *Mol. Biol. Cell* **14**:2984-2998.

Vogt A, Pestell KE, Day BW, Lazo JS and Wipf P (2002) The antisignaling agent SC-ααδ9, 4-(benzyl-(2-[2,5-diphenyloxazole-4-carbonyl)amino]ethyl)carbamoyl)-2-decanoylaminobutyric acid, is a structurally unique phospholipid analogue with phospholipase C inhibitory activity. *Mol. Cancer Therap.* **1**:885-892.

Vogt A, Rice RL, Settineri CE, Yokokawa F, Yokokawa S, Wipf P and Lazo JS (1998) Disruption of insulin-like growth factor-1 signaling and down-regulation of Cdc2 by SC-ααδ9, a novel small molecule antisignaling agent identified in a target array library. *J. Pharmacol. Expt. Therap.* **287**:806-813.

Wang H-M, Mao Y, Chen AY, Zhou N, LaVoie EJ and Liu L (2001) Stimulation of topoisomerase II-mediated DNA damage via a mechanism involving protein thiolation. *Biochem.* **40**:3316-3323.

Molecular Pharmacology Fast Forward. Published on July 1, 2004 as DOI: 10.1124/mol.104.001784
This article has not been copyedited and formatted. The final version may differ from this version.

FOOTNOTES

Supported in part by NIH grants CA50771, CA52995, CA78039, CA90787, GM065805 and the Fiske Drug Discovery Fund.

To whom request for reprints should be addressed: Department of Pharmacology, University of Pittsburgh, E1340 Biomedical Science Tower, Pittsburgh, PA 15261-0001; Email: lazo@pitt.edu

Molecular Pharmacology Fast Forward. Published on July 1, 2004 as DOI: 10.1124/mol.104.001784
This article has not been copyedited and formatted. The final version may differ from this version.

FIGURE LEGENDS

Figure 1. Chemical structures of cyclopentaquinoline analogs with their corresponding IC_{50} concentrations against recombinant full length human Cdc25B.

Figure 2. Kinetic analysis of Cdc25A inhibition by 5661118. Lineweaver-Burk plot of 5661118 inhibition of Cdc25A catalytic domain illustrating mixed partial inhibition. Results are mean ± SEM (n = 3).

Figure 3. Chemical structures and Cdc25B phosphatase inhibition by naphthofuranediones. Panel A. Chemical structures of two naphthofuranediones. Panel B. Concentration response curve for 5169131. Panel C. Concentration response curve for 5169133. Recombinant full-length human Cdc25 phosphatases were incubated with various concentrations of 5169131 and 5169133 at room temperature for 60 min. Fluorescence emission from the product was measured with a multiwell plate reader as described in the Materials and Methods Section. Results are mean ± SEM (n = 4).

Figure 4. 5169131 is a competitive and reversible inhibitor of Cdc25B. Panel A. Kinetic analysis of 5169131 inhibition of full-length human recombinant Cdc25B. The Lineweaver-Burk plot demonstrates competitive inhibition. Results are representative of 2 separate experiments. Panel B. Reversibility of Cdc25B inhibition with 5169131. Recombinant Cdc25B was pre-incubated with 3 x the IC_{50} value of DA-3003-1 (2.5 μM) or 5169131 (30 μM) for 0, 5 or 20 min in the absence of the substrate and then diluted ten-fold and assayed for enzyme activity. Results are mean ± SEM (n = 3).

Molecular Pharmacology Fast Forward. Published on July 1, 2004 as DOI: 10.1124/mol.104.001784
This article has not been copyedited and formatted. The final version may differ from this version.

Figure 5. G_2/M arrest by 5169131. tsFT210 cells were cultured at the permissive temperature of 32^{o}C and then incubated for 17 h at the nonpermissive temperature (39.4^{o}C). DMSO or drug was added to cells for an additional 6 h at 32^{o}C. Panel A. Asynchronous control. Panel B. G_2/M arrested cells after temperature shift for 17 h at 39.4^{o}C. Panel C. DMSO treated cells. Panel D. Cells treated with 1 μM nocodazole (positive control). Panel E-H. Cells treated with 1-30 μM 5169131. Data are representative of two independent experiments.

Figure 6. Effect of 5169131 on Cdk1 phosphorylation status and Cdk1 kinase activity. G_2/M arrested tsFT210 cells were released for 1 h in the presence of various concentrations of 5169131 or DMSO vehicle followed by immunoprecipitation with anti-Cdk1 mouse monoclonal antibody. Panel A. Western blot probed with phospho-Cdk1 (Tyr15) antibody. Phospho-Cdk1 bands were normalized to total Cdk1 levels (loading control) by densitometry and then divided by the DMSO control value to determine fold increase over DMSO. Panel B. Kinase activity assay with Cdk1/cyclin B kinase incubated with DMSO vehicle, roscovitine, or 5169131 using Histone H1 as a substrate. 5169131 caused a concentration-dependent increase in hyperphosphorylation of Cdk1 in cells and did not affect Cdk1 kinase activity *in vitro*.

Figure 7. G_1 phase arrest by 5169131. tsFT210 cells were cultured at the permissive temperature of 32^{o}C and then incubated at the nonpermissive temperature (39.4^{o}C) for 17 h as described in Figure 6. Cells were then released for 4-6 h at 32^{o}C to arrest cells at the G_1 checkpoint. DMSO or drug was added for an additional 6 h at 32^{o}C. Panel A.

Molecular Pharmacology Fast Forward. Published on July 1, 2004 as DOI: 10.1124/mol.104.001784
This article has not been copyedited and formatted. The final version may differ from this version.

Asynchronous control. Panel B. G_2/M arrested cells after temperature shift for 17 h at 39.4^{o}C. Panel C. G_1 arrested cells after temperature shift back to 32^{o}C. Panel D. DMSO treated cells. Panel E. Cells treated with 50 μM roscovitine (positive control). Panel F-I. Cells treated with 1-30 μM 5169131. Data are representative of two independent experiments.

Figure 8. Growth inhibitory effects of 5169131 in human PC-3 prostate cells, MDA-MB-435 breast cancer cells, parental human leukemia K562 cells and VP-16 resistant K/VP.5 cells containing reduced levels of DNA topoisomerase IIα. Panel A. MDMA-MB-435 and PC-3 cells were treated with vehicle or 5169131 for 96 h and nuclei were enumerated by automated batch image acquisition and analysis. Data were normalized to expansion of vehicle-treated cells over a 4 day period and represent the averages of 4-5 independent experiments $\pm$ SEM. Panel B. K562 and K/VP.5 cells were treated with 5169131 for 48 h prior to assessment of growth inhibition by counting cells on a model ZBF Coulter counter. The extent of growth in drug-treated versus control cells was expressed as percent inhibition of control growth. Results shown are composites from three separate experiments performed on separate days. 5169131 inhibited proliferation of these cell lines and was unaffected by differing levels of DNA topoisomerase IIα.

Figure 9. Panel A. Superposition of the molecular models for bound conformations of the 5169131 inhibitor and the OMFP substrate obtained independently with the catalytic domain of Cdc25B illustrating the close overlap between their binding sites, consistent with their competitive binding. Based on the model, 5169131 binds to the groove that

extends from the catalytic side. The Cdc25B backbone is shown in yellow, OMFP and 5169131 are represented as ball and stick models. Atoms are colored gray (C), red (O), yellow (S), green (Cl), blue (N) and purple (PO_4). The figure was obtained using the MOE program (Chemical Computing Group Inc.). Panel B. Conformation of the inhibitor 5169131 (stick representation) at the binding cavity of the Cdc25B protein represented as Connolly surface. Color index: red exposed, green hydrophobic and blue hydrophilic.

Figure 10. Molecular model of the interaction of 5169131 and 5169133 with the amino acids in the binding cavity adjacent to the Cdc25B catalytic site. Panel A. Interactions of 5169131 with the side chains of amino acids R482, R544 and Y428. Panel B. The 5169133 congener differs from 5169131 by the substitution of a hydrogen atom with a bromine, which is predicted to violate the van der Waals radius of the Cγ atom belonging to the spatially neighboring amino acid T547 of Cdc25B. Atoms are colored gray (C), red (O), blue (N) and brown (Br). The MOE program (Chemical Computing Group Inc.) was used to obtain the figure.

Molecular Pharmacology Fast Forward. Published on July 1, 2004 as DOI: 10.1124/mol.104.001784
This article has not been copyedited and formatted. The final version may differ from this version.

Table 1A. Cell cycle analysis of G_2/M arrested tsFT210 cells treated with 5169131. Data are the mean of two individual experiments ± range.

Cell Treatment	%G_1	%S	%G_2/M
Asynchronous	23 ± 4	53 ± 5	24 ± 1
G_2/M arrest	1 ± 1	18 ± 3	81 ± 4
DMSO	60 ± 10	19 ± 11	21 ± 1
1 μM Nocodazole	2 ± 2	18 ± 8	80 ± 10
30 μM 5169131	9 ± 3	20 ± 9	71 ± 6
20 μM 5169131	16 ± 4	23 ± 6	61 ± 3
10 μM 5169131	43 ± 11	21 ± 6	36 ± 4
1 μM 5169131	58 ± 12	21 ± 12	21 ± 1

Table 1B. Cell cycle analysis of G_1 synchronized tsFT210 cells treated with 5169131. Data are the mean of two individual experiments ± range.

Cell Treatment	%G_1	%S	%G_2/M
Asynchronous	23 ± 2	57 ± 1	20 ± 1
G_1	59 ± 16	21 ± 12	20 ± 4
DMSO	17 ± 5	69 ± 11	14 ± 7
30 μM 5169131	44 ± 9	36 ± 1	20 ± 10
20 μM 5169131	28 ± 7	52 ± 2	20 ± 10
10 μM 5169131	17 ± 3	68 ± 5	15 ± 2
1 μM 5169131	19 ± 4	71 ± 11	10 ± 7

Table 1

	IC50 (μM)		IC50 (μM)
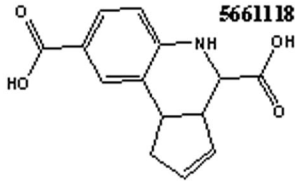 5661118	2.5	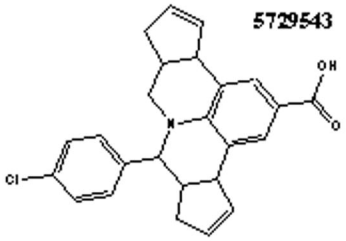 5729543	>100
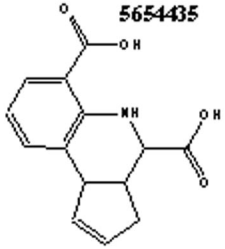 5654435	4.5	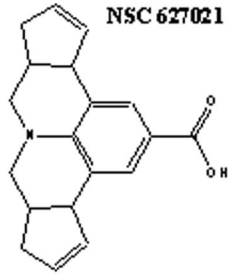 NSC 627021	>100
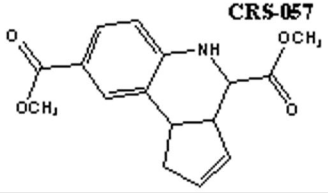 CRS-057	>100	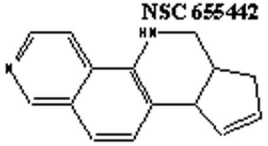 NSC 655442	>100
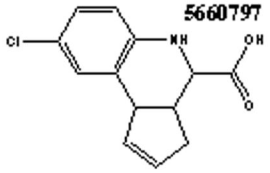 5660797	29	 NSC 604519	>100

Figure 1

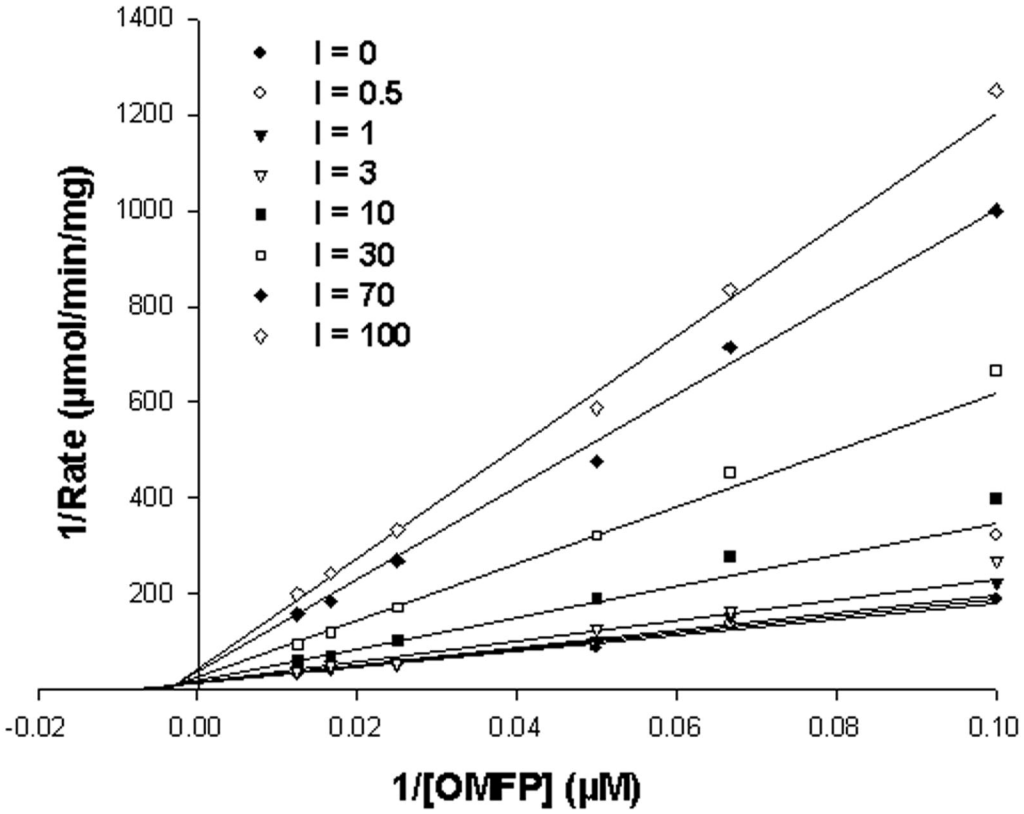

Figure 2

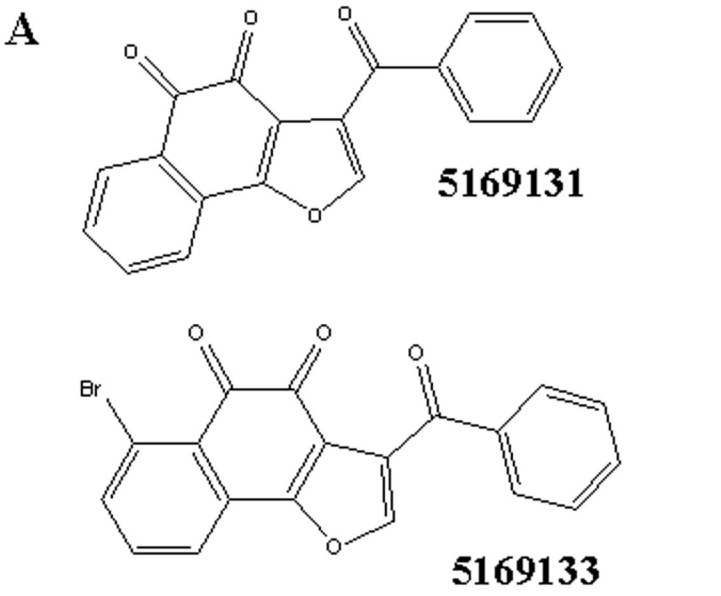
A
5169131
Br
5169133

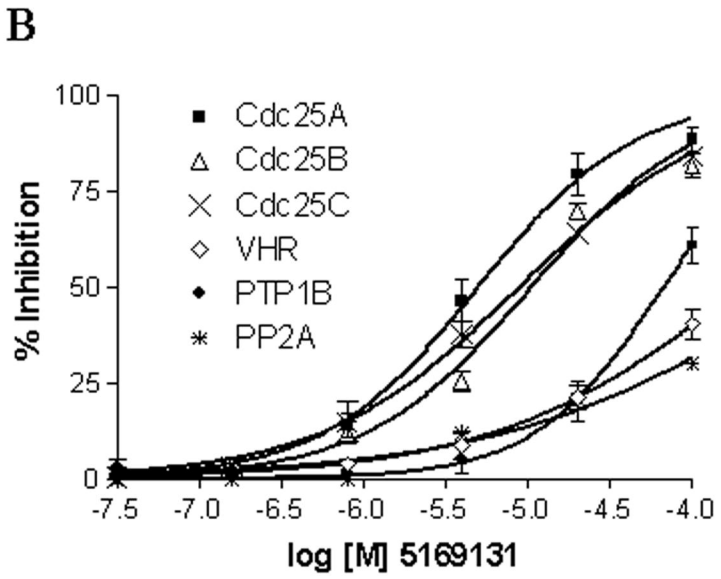
B
100
75
50
25
0
% Inhibition
Cdc25A
Cdc25B
Cdc25C
VHR
PTP1B
PP2A
-7.5
-7.0
-6.5
-6.0
-5.5
-5.0
-4.5
-4.0
log [M] 5169131

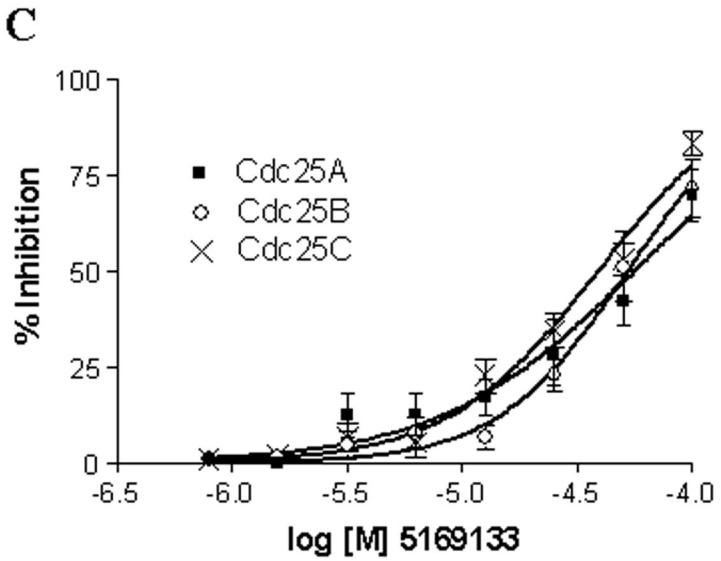
C
100
75
50
25
0
% Inhibition
Cdc25A
Cdc25B
Cdc25C
-6.5
-6.0
-5.5
-5.0
-4.5
-4.0
log [M] 5169133

Figure 3

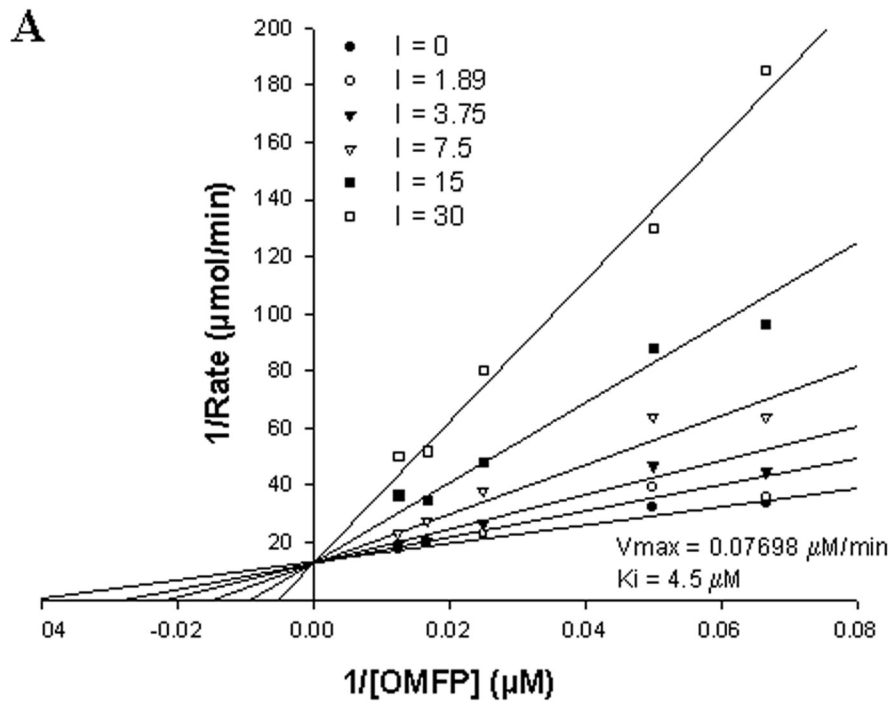

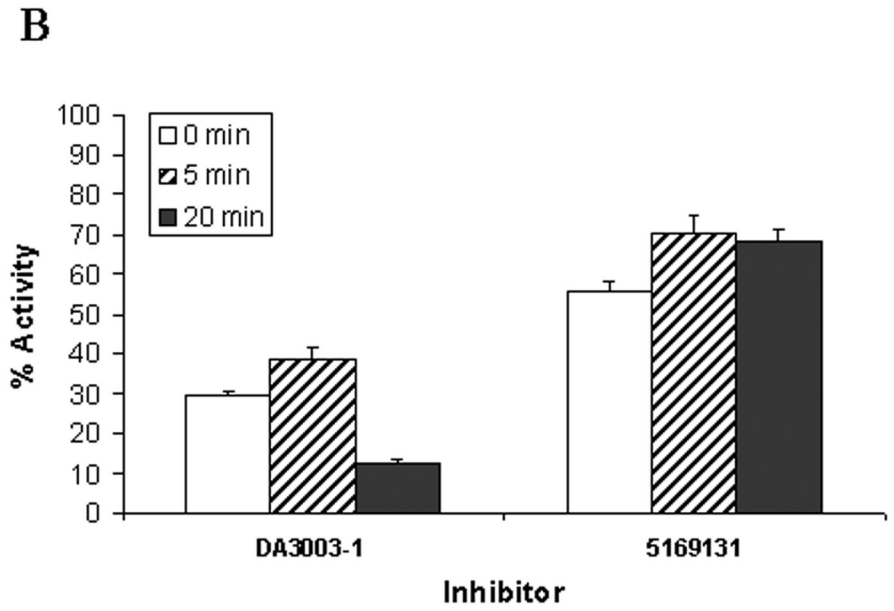

Figure 4

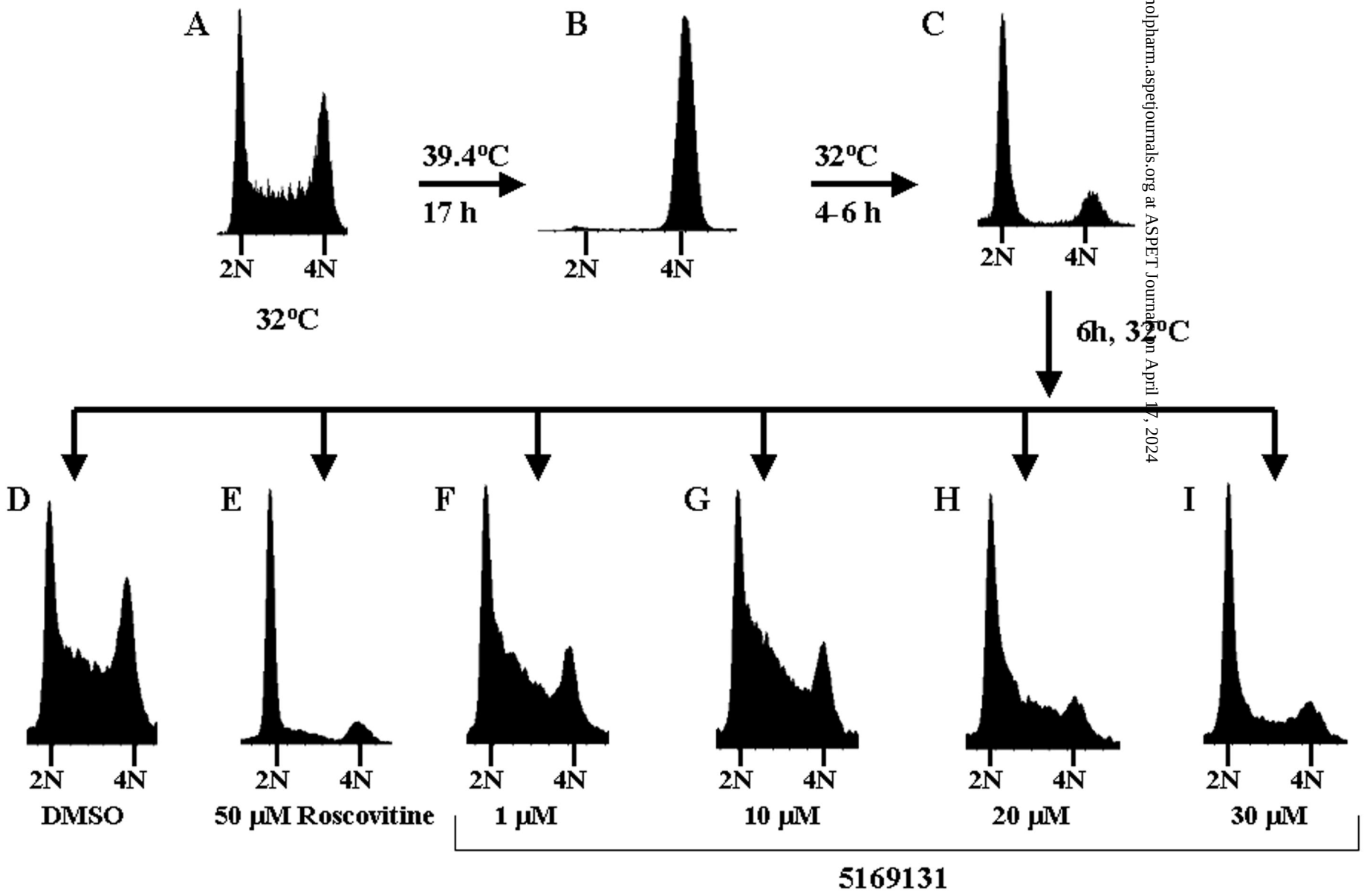

Figure 5

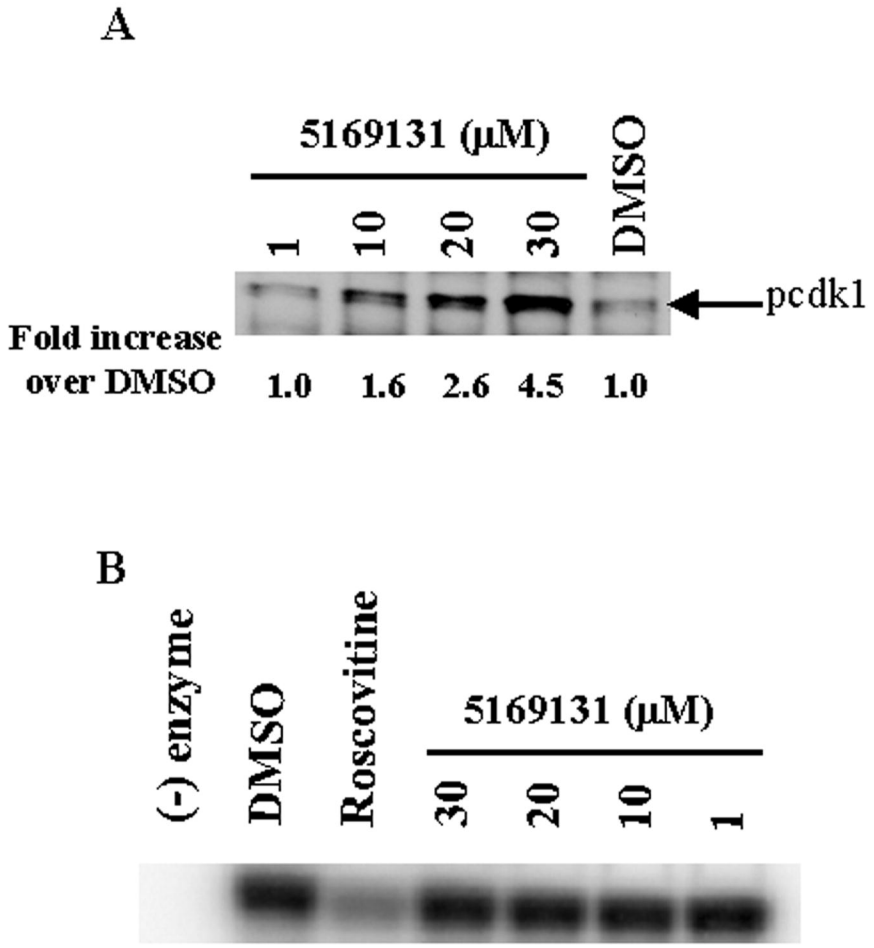

Figure 6

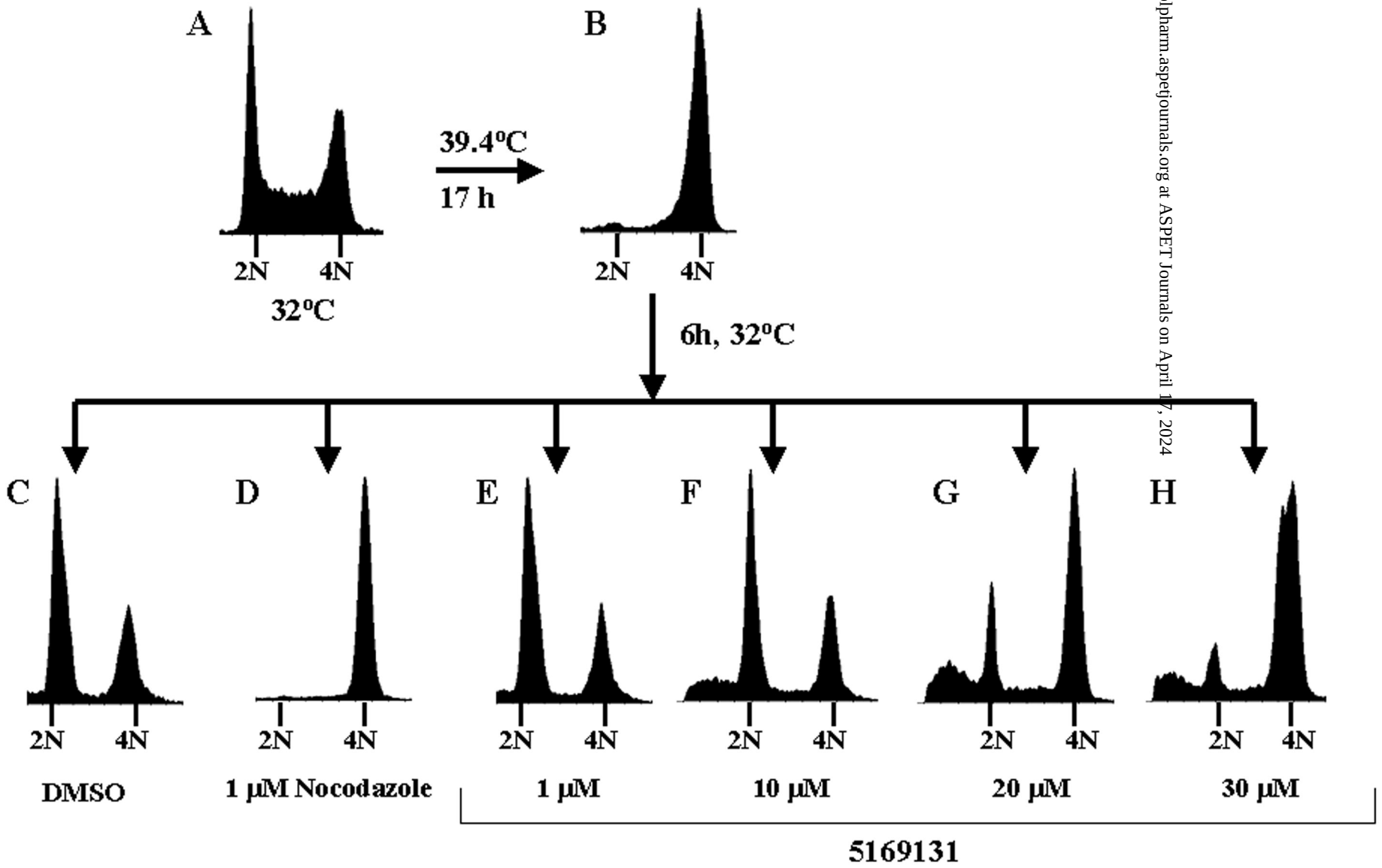

Figure 7

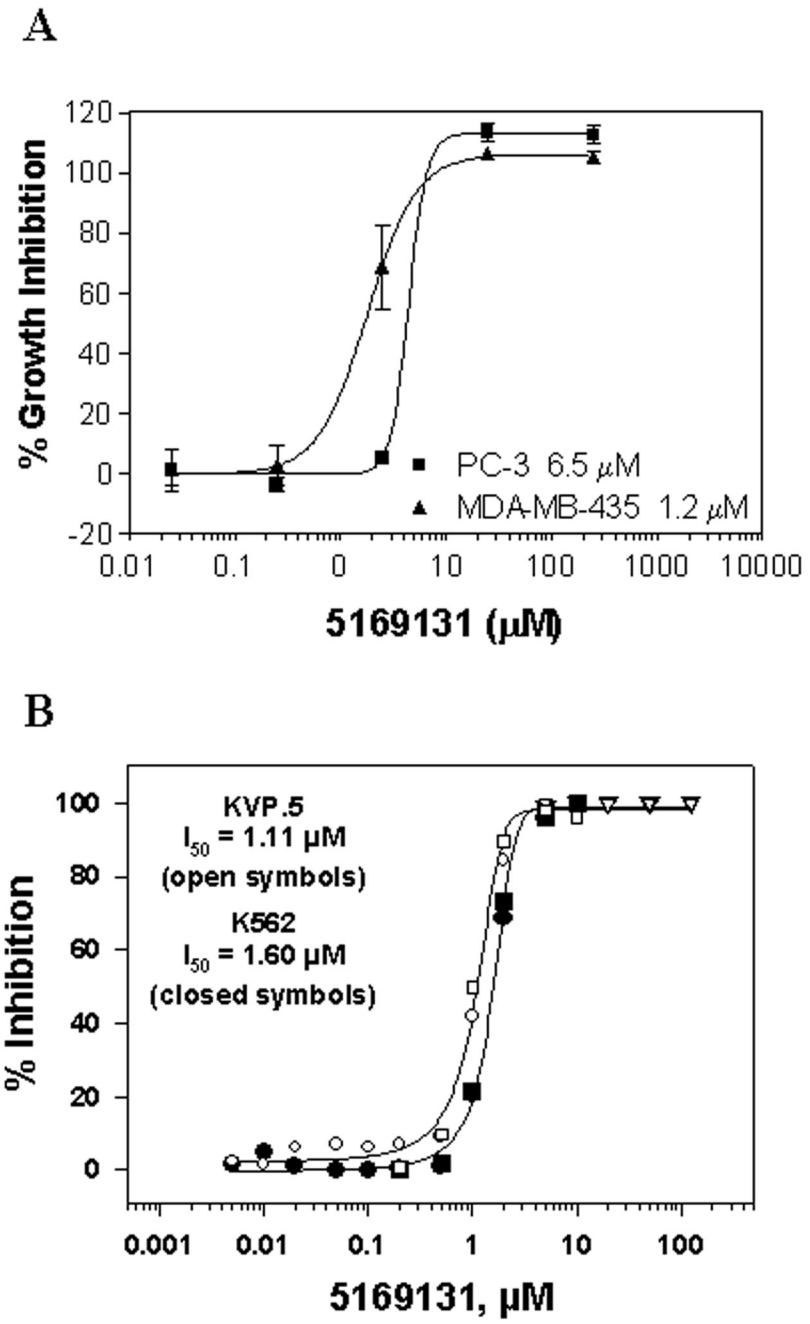

Figure 8

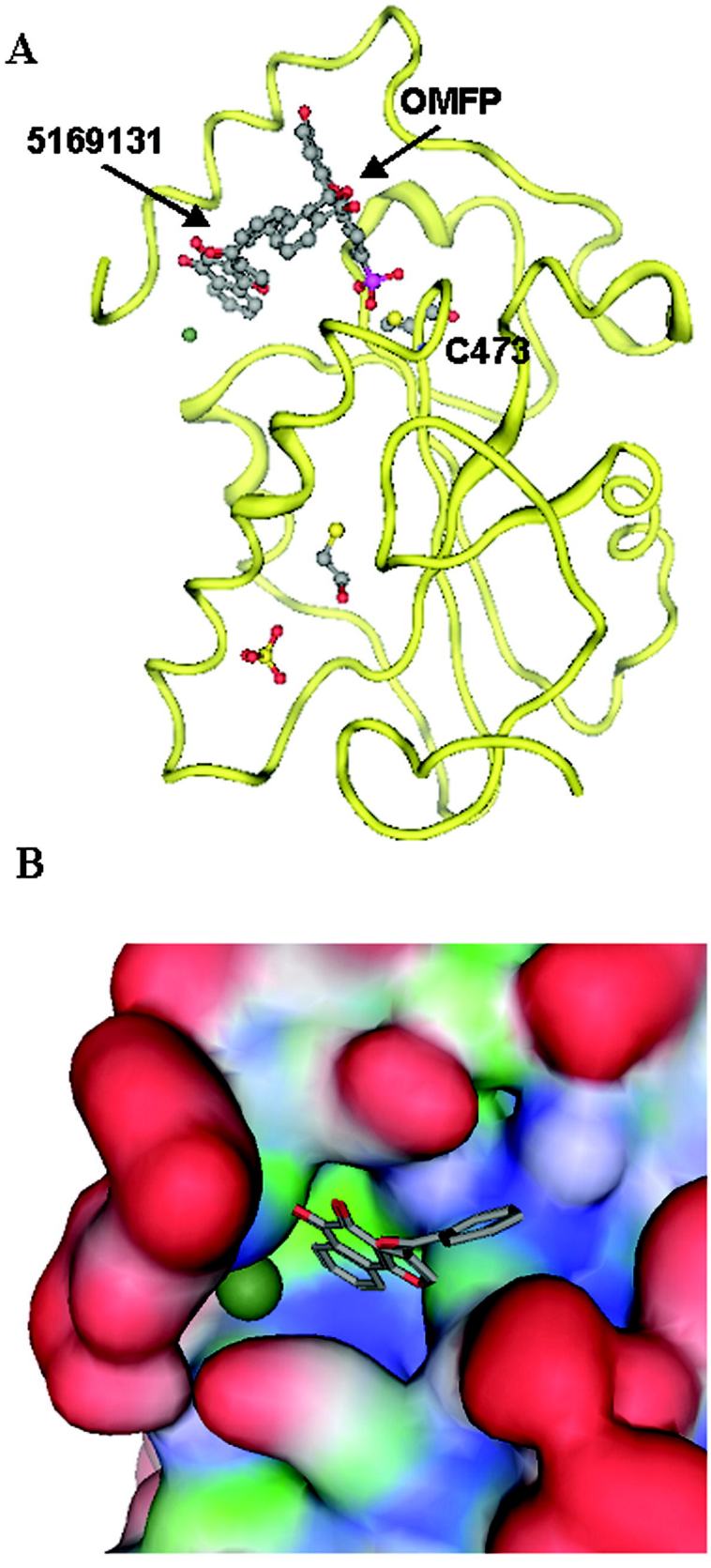

Figure 9

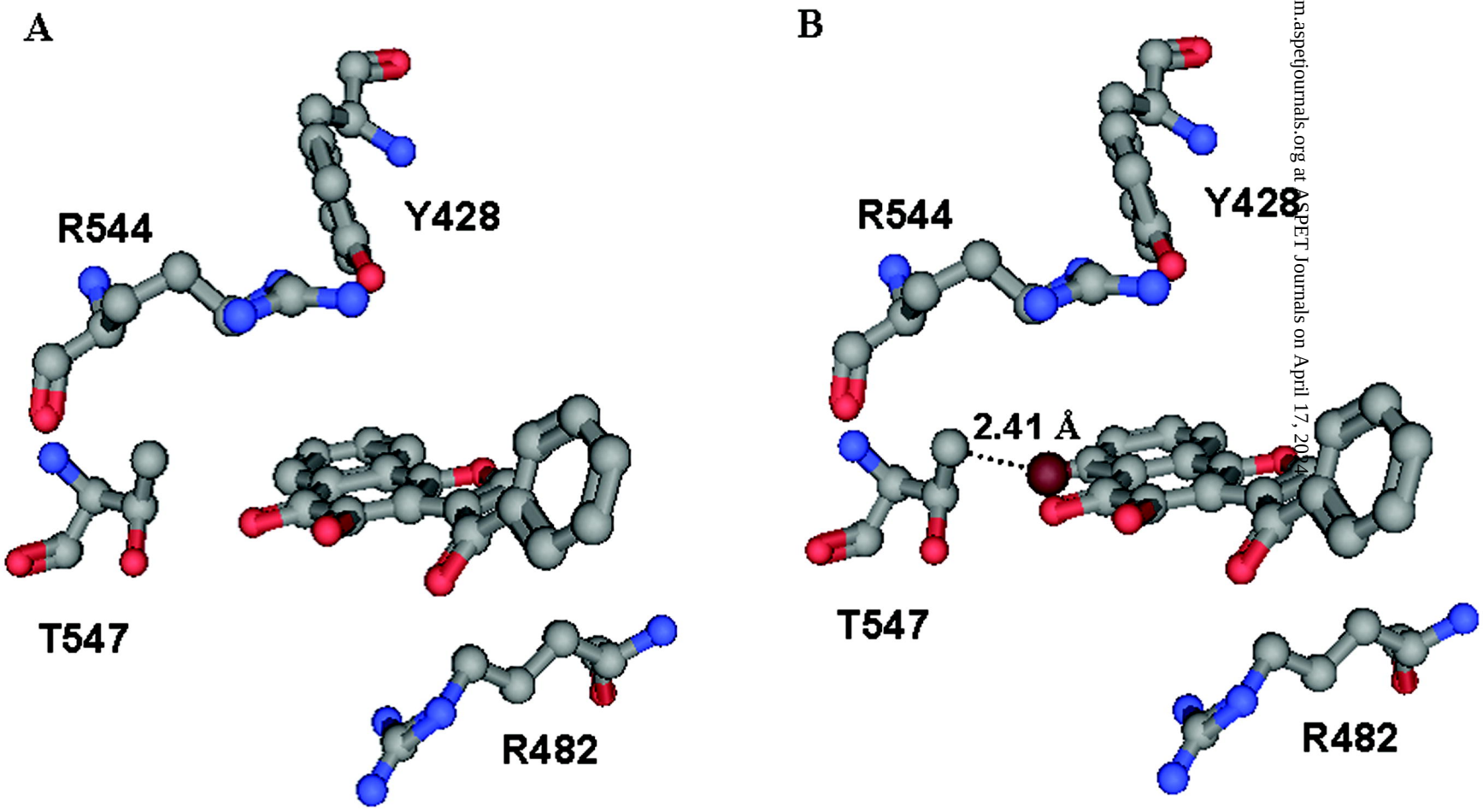

Figure 10